ROYAL SOCIETY
OF CHEMISTRY

PAPER

Check for updates

Effect of pre-treatment of herbaceous feedstocks on behavior of inorganic constituents under chemical looping gasification (CLG) conditions

Florian Lebendig [ID] * and Michael Müller

Biomass chemical looping gasification (BCLG) is a promising key technology for producing carbon neutral liquid biofuels. However, various ash-related issues, such as bed agglomeration, fouling and slagging, or high-temperature corrosion may cause significant economic and ecologic challenges for reliable implementation of BCLG. Biomass pre-treatment methods, such as torrefaction, (water-)leaching and combination of both approaches may significantly improve ash-related characteristics and therefore provide a promising approach for enabling the use of herbaceous residues. This study deals with essential lab-scale investigations under well-defined, gasification-like conditions at 950 °C, joint with thermo-dynamic equilibrium calculations. Fundamental knowledge on the influence of pre-treatment methods on the release and fate of volatile inorganics as well as on the ash melting behavior of the residual ashes was gained. Molecular Beam Mass Spectrometry (MBMS) was applied for *in situ* online hot gas analysis of (non-)condensable gas species during gasification of pre-treated feedstocks. Both ash composition and behavior were characterized particularly by X-ray powder diffraction method and hot stage microscopy (HSM). The results obtained by chemical characterization were taken into account for thermodynamic modelling. Based on the results, conclusions were drawn on how different pre-treatment technologies can help to improve and solve ash-related issues during thermochemical conversions. It has been demonstrated that (combined) pre-treatment methods can counteract the above-mentioned problems and have a noticeable effect on the principal inorganic constituents (*e.g.* K, Ca, Si) originating from the ash by shifting their proportions.

1. Introduction

In the last decade, the energy demand worldwide has increased as a result of the population growth and is still predominantly covered by fossil-based fuels. However, countries are progressively pushing the expansion of environmentally friendly, renewable energies.[1] In order to limit global warming to 2 °C or even 1.5 °C, carbon emissions from energy conversion are required to reach net zero by around mid-century.[2] Biofuels are in contrast to conventional, fossil-based fuels considered as carbon neutral alternatives for regenerative energy or syngas production. Biomass-based fuels are promising candidates as the CO_2 produced during combustion has previously been removed from the atmosphere *via* photosynthesis, and the emitted CO_2 can potentially be considered as neutral.[3] Moreover, the topographical independence and comparatively ample availability makes biomass a promising candidate over other renewable energy sources such as wind, solar or hydroelectric storage.[4]

A promising key technology for converting biomass into sustainable synthetic fuels is chemical looping gasification (CLG), which represents an important part of the thermo-chemical Biomass-to-Liquid (BtL) route. The entire multistep process can be seen elsewhere.[5] Fig. 1 illustrates the principle of the BCLG process, where the overall air/fuel ratio is $\lambda < 1$.

Fig. 1 Schematic sketch of the BCLG process: the reduced oxygen carrier is circulated to the air reactor to be reoxidized before a new cycle starts. The exothermic heat resulting from the metal reaction with oxygen provides endothermic energy ΔT which is necessary for the fuel reactor operation.

Forschungszentrum Jülich GmbH, Institute of Energy and Climate Research (IEK-2), Wihelm-Johnen Straße, 52428 Jülich, Germany. E-mail: f.lebendig@fz-juelich.de

The process is divided into two parts, the air reactor, where the oxygen carrier is oxidized, and the fuel reactor, where the gasification takes place and syngas is produced.

During the gasification itself, however, various biomass-based, ash-related issues can cause operational problems. Generally, it can be stated that ash-related issues for biomass gasification systems are assumed to be largely similar to those for combustion,[6] however, regarding their explicit behavior under gasification-like conditions, new biomass fuels are not well-defined yet. Therefore, a comprehensive fuel characterization with focus on gasification-related fuel properties is regarded as a necessary part for their introduction. A fundamental knowledge of inorganic, biomass-derived constituents is required in order to understand their impact on the chemical looping gasification process, such as high-temperature corrosion, bed agglomeration, fouling and slagging, oxygen carrier poisoning or pollutant emissions.

Biomass, especially fast-growing species such as herbaceous plants contain in general a high amount of chlorine in contrast to fossil fuels (e.g. coal), which has in turn a negative effect on the behavior of metal components, e.g. the rector wall unit.[7] This phenomenon is understood as chlorine-induced corrosion, which is known to be the most important corrosion process in power plants, firing waste, coal and/or biomass.[8] Besides the corrosion risk, chlorine promotes the formation of hydrogen chloride, which causes acidification[9] and dioxins, resulting in a risk to the human health because of their toxicity, persistence, and lipophilicity-based bio-accumulation.[10,11] Alkali metal compounds (mainly potassium and sodium) are known to form problematic eutectic melts on different surfaces through promotion of low-melting silicates,[12] whereas sulfur may react to cause sulfidation of the reactor material components, and so forth. Consequently, the amount of formed slag increases, consequently accelerating bed agglomeration issues.

Likewise, the phenomenon of fouling and slagging is typically caused by alkali salts,[13] mainly by chlorides, carbonates or sulfides. It is noteworthy to mention that the nature of biomass has a strong impact on the ash melting behavior.

In order to enable or improve the use of low-grade biomass fuels for thermochemical bioenergy applications, pre-treatment methods may be viewed as essential steps. Several biomass upgrading approaches are regarded as necessary process steps for thermochemical conversion of biomass and the energy utilization.[14,15] For example, the torrefaction process can be considered as a mild form of pyrolysis, in which biomass is heated up to temperatures of typically 200–300 °C in absence of oxygen. Torrefaction converts biomass into a coal-like material and, despite a lower content of volatile components, torrefied biomass ignites faster than untreated raw material.[16] The thermal treatment aims to evaporate not only all water contained in the feedstock, but also a part of volatile compounds, e.g. chlorine,[17] which has generally a significant effect on the release and transformation of the alkali and alkaline earth metals.[18,19] Some part of chlorine releases to the gas phase during torrefaction, and organochlorine (C–Cl) compounds are formed, mostly in form of methyl chloride.[17,20]

Previous investigations in[21] also indicated that sulfur in biomass was significantly released by torrefaction, and the decrease in Cl and S content was likely to suppress the chlorides/sulfates-induced fouling deposition. Due to an increased density of the material, torrefaction provides in turn a higher calorific value. Likewise, the bulk density, grindability, and hydrophobicity can be effectively improved, reducing the costs associated with biomass transportation, storage, and handling.[22–24]

Alkali metal salts can easily be removed by leaching the feedstock with water due to their high solubility. Tukey[25] defined leaching as the removal of substances (inorganic and organic) from plants by aqueous solutions including rain, dew, mist, and fog. For gasification process, proceeding at elevated temperatures (typically >800 °C), several different problems such as ash fouling or environmental impacts can be reduced by systematic modification of the fuel composition. In particular, alkali metal cations such as potassium and sodium as well as their corresponding alkali salts KCl/NaCl, but also sulfates and carbonates are proven to be problematic species. In a previous study performed by Meesters et al.,[26] extraction experiments exhibited that both chlorine and potassium concentration can be reduced by 80% respectively 90% after four consecutive extraction steps with water, bringing chlorine and potassium down or close to acceptable levels. An in-depth study in 1996[27] characterized the effect of aqueous extraction of inorganic constituents on straw ash fusibility. It was found that without leaching, the ash was observed to fuse between 900 °C and 1000 °C. However, no ash fusion was observed with well-leached samples at temperatures up to 1600 °C. The aforementioned outcomes emphasize that leaching biomass is one effective approach which is known to improve fuel properties or affecting some physico-chemical parameters of the formed leachates.[28] Insoluble inorganic components are not removed by water-leaching because they are differently, particularly the cations are mostly bound with active sites of lignin, cellulose, or hemicellulose, and in order to remove them, an acidic environment is required, e.g. HCl.[29,30]

Most research is focused on analyzing fuel properties solely by leaching or (dry and wet) torrefaction,[31–33] however, there are only few studies on the combination of those methods presented yet.[34] Therefore, fundamental knowledge on applied biomass pre-treatment methods, such as thermal treatment (torrefaction), water-leaching and combination of both approaches should be provided in order to estimate operational risks. Several investigative techniques have been applied in order to understand the influence of pre-treatment methods. Molecular Beam Mass Spectrometry (MBMS) was employed to investigate the release and fate of inorganic volatile species during gasification. Ashes were characterized by X-ray diffraction (XRD) and ash fusion test. Lab-scale experiments were complemented by thermodynamic modelling using FactSage software in order to predict release and condensation of volatile species and phase transformation in the ash. Based on the obtained results, specific conclusions about the risk of bed agglomeration, slagging and fouling and high-temperature corrosion could be drawn.

2. Materials and methods

2.1. Materials, pre-treatment and chemical characterization

The four commercially purchased (Futtermittel Louven, Erftstadt, Germany) herbaceous feedstocks wheat, barley, corn, and colza straw were selected as biomass-based fuels in this study, because of their availability and potential use in Europe or worldwide in general. Different pre-treatment methods were applied, and the sample abbreviations specified in this study are denoted as follows: the aforementioned straw varieties were torrefied (To), water-leached (WL), and both steps were combined, taking into account the order (either To-WL or WL-To).

The samples were washed twice; each washing cycle lasted one hour and the sample-water mixture, consisting of 50 g biomass and 0.5 l deionized water, was constantly mixed during this time. After each washing step, the samples were vacuum filtrated and rinsed with a small amount of deionized water. After the washing process, the samples were kept 24 h for drying inside of a fume hood.

For the thermal pre-treatment, a dry torrefaction method without water steam was applied, and the samples were torrefied in pure argon atmosphere at 250 °C for 1 h. The torrefaction grade was 27% for barley straw, 37% for colza straw, and 28% for both wheat and corn straw on average. The moisture content was 7% for barley straw, 10% for colza straw, 6% for wheat straw, and 8% for corn straw on average.

Each sample was chemically characterized afterwards, and the ash content was determined gravimetrically (550 °C, 1.013 bar, 36 h, constant mass). The samples were analyzed on their elemental composition with a CHNS analyzer and optical emission spectroscopy combined with inductively coupled plasma (ICP-OES) for the major ash forming elements. Microwave acid digestion of the fuels was applied prior to the determination by ICP-OES. This option was preferred in order to avoid the volatilization of substances caused by pre-treatment in a muffle furnace. Each fuel sample was milled and sieved relating to a diameter of 0.56 mm to improve analytical investigations in further steps.

2.2. Experimental hot gas analysis by molecular beam mass spectrometry (MBMS)

Molecular Beam Mass Spectrometry (MBMS) was applied for the real-time determination of inorganic gaseous species released during gasification. The apparatus allows studies of hot gases from diverse origins in biomass-derived feedstocks under a gasification-like atmosphere. The general technique of the MBMS is based on common mass spectrometry, which analyzes the mass–to–charge ratios (m/z) in an electromagnetic field. A detailed description of the experimental setup of the MBMS can be found elsewhere.[35,36]

Release experiments under gasification-like conditions at 950 °C were performed. A four-zone furnace was employed, and the alumina-tube inside the furnace was directly connected to the MBMS nozzle, which represents the gas inlet of the apparatus. The gasification of the sample took place within the first two zones at 950 °C. The third temperature zone was set at 1400 °C to crack all formed hydrocarbons, as only inorganic species should be investigated. The setup of the tube furnace can be seen in other publications.[35,36]

In total, three measurements for each sample were realized and averaged for semi-quantitative analyses and error calculations. The same atmospheric conditions as for the ashing procedure (section 2.4.) were used throughout the measurement campaign, i.e., 15 vol% H_2O-steam and 5 vol% CO_2 in He (to increase sensitivity of the MBMS). The total gas flow was set to 4 L min^{-1} for each experiment. Then, 50 mg of fuel was gasified in a single run. The samples were kept in the furnace for varying retention times, depending on the first overview of all spectra, from 2 min to max. 6 min and were characterized afterwards. The retention time reflects the reaction sequence, as species show different release behavior or, more precisely, only devolatilization or subsequent char gasification and ash reaction. Intensity-time profiles of $^{23}CO_2^{++}$, $^{34}H_2S^+$, $^{35}Cl^+$, $^{36}HCl^+$, $^{37}Cl^+$, $^{38}HCl^+$, $^{39}K^+$, $^{47}PO^+$, $^{55}KO^+$, $^{58}NaCl^+$, $^{60}COS^+$, $^{62}P_2^+$, $^{63}PO_2^+$, $^{64}SO_2^+$, $^{74}KCl^+$, $^{81}Na_2Cl^+$, $^{97}NaKCl^+$, $^{126}P_2O_4^+$, $^{113}K_2Cl^+$ and $^{142}P_2O_5^+$ were recorded and normalized to the $^{23}CO_2^{++}$ base level signal for quantification.

2.3. Ash sample preparation for ash fusion tests and X-ray powder diffractometric analysis

Ash of each feedstock sample was produced under gasification-like conditions at constant temperature (550 °C). The gasifying medium comprised 15 vol% H_2O-steam in N_2, and 5 vol% CO_2 was added as substitution for the oxygen carrier. At the beginning of the procedure, a small amount of oxygen was added to accelerate the carbon conversion. A lambda sensor was used during the ashing procedure for controlling the partial pressure of oxygen. When the partial oxygen pressure increased, the ashing procedure was almost completed and the oxygen supply was stopped to prevent oxidizing conditions or combustion. Afterwards, the ash samples were annealed at 550 °C for 3 h in an argon-hydrogen (Ar/4% H_2) atmosphere to enhance formation of crystalline compounds. The detection of crystalline compounds is indispensable for X-ray diffractometric investigation.

For the determination of ash melting behavior by hot stage microscopy, 120 mg ash was pressed into a cylindrical pellet with a diameter of 5 mm (the strength was set constantly to 1.5 kN). One drop of pure isopropanol was added as surfactant to keep the pellet stable during the pressing process. The sample pellet height varied between 4 mm to 7 mm. Note that the same amount of ash was weighed for each sample preparation.

2.4. Ash fusion tests by hot stage microscopy (HSM)

The determination of the melting behavior of the fuel ashes was performed by hot stage microscopy. The typical sample geometry is represented by a cylindrical pellet (section 2.3.), which is placed inside of a tube furnace. The furnace chamber was flushed with a constant flow of 13 vol% carbon dioxide and 87 vol% argon. Based on preliminary equilibrium calcu-

lations, the defined amount of carbon dioxide was required to keep possibly formed carbonates stable. The furnace was heated from room temperature up to 1300 °C at 5 K min^{-1}. A CCD camera was placed behind the furnace outlet, and photos were taken at every degree Celsius. A corresponding software evaluated the change of the sample shape (height ratio of the pellet) in dependence of the temperature change. Depending on this information, conclusions can be drawn about the ash melting behavior. The evaluation is based on the ratio of current sample height/original sample height (coefficient h_x/h_0) according to Pang *et al.*[37]

2.5. Thermodynamic modelling

Thermodynamic equilibrium calculations, which are based on the minimization of Gibbs free energy, were realized in order to predict inorganic phase formation of ash constituents under gasification-like conditions, using the computational package FactSage™ 7.3.[38] The commercial database SGPS has been used for pure gaseous and some solid stoichiometric compounds. Additionally, the database GTOX, which has been developed in cooperation by Forschungszentrum Jülich and GTT-Technologies was considered for the present study.[39] The chemical composition of the corresponding fuel ashes was taken into account for thermodynamic equilibrium calculations (Table 1). Phase formations under pyrolysis conditions were calculated without addition of steam and oxygen, whereas the phase formations under gasification conditions expected for CLG[34] were calculated in consideration of adding water (steam/feedstock = 0.5 g/g) and oxygen (Fe_2O_3/feedstock = 0.48 g/g, only the oxygen of the oxygen carrier Fe_2O_3 was taken into account). It shall be noted here that the latter assumes a full reduction of a completely oxidized oxygen carrier, which is likely not the case in the real process. However, the effectively supplied amount of oxygen is similar, so that a reasonable syngas composition was achieved.

3. Results

3.1. Experimental investigations

3.1.1 Fuel composition. The results of the ultimate analysis of each feedstock are listed in Table 1. Basically, torrefied samples show a higher weight percentage of inorganic species compared to the source material itself. In contrast to the other straw varieties, corn ash showed a higher average concentration of Mg and Si, which might be explained on account of the fact that corn straw was certainly contaminated with soil impurities.

The torrefaction process increases the density of the material which means that it eliminates volatile organic compounds and water (in form of moisture). This in turn increases the fixed carbon content, and subsequently amplifies the calorific value of the feedstock.[40,41] Water-leaching decreases the Cl content noticeably, whereas no effect is observed on the Si content due to its insolubility. Since potassium is mainly found in form of highly soluble salts as KCl in the fuel, water-

Table 1 Ultimate analysis of pre-treated fuel samples (wheat, barley, colza and corn straw)

wt%	Wheat	To	WL	To-WL	WL-To
C	43.8	50.5	45.2	49.3	51.3
H	6.18	5.83	6.39	5.83	5.96
N	0.39	0.44	0.3	0.47	0.34
O	44.2	37.0	45.4	39.4	39.2
S	0.18	0.17	0.1	0.1	0.1
mg kg^{-1}		Ash components (major elements only)			
Cl	3360	424	127	298	113
Al	20	20	20	61	20
Ca	2010	1747	340	2640	845
Fe	10	7	7	76	7
K	13 000	17 840	2360	6400	3214
Mg	468	716	248	588	358
Na	90	90	90	200	90
P	220	1293	78	210	96
Si	7840	10 130	7410	10 200	10 640

wt%	Barley	To	WL	To-WL	WL-To
C	43.4	50.3	44.3	47.1	49.5
H	6.2	5.91	6.37	5.85	5.95
N	0.56	0.73	0.39	0.37	0.63
O	43.8	37.7	44.7	39.7	40.2
S	0.13	0.12	0.1	0.1	0.1
mg kg^{-1}		Ash components (major elements only)			
Cl	618	1076	42	60	100
Al	20	20	20	40	20
Ca	3010	4310	2820	4400	4130
Fe	7	7	7	49	7
K	15 600	19 550	3600	7170	4610
Mg	377	550	271	515	405
Na	90	140	90	200	90
P	890	1258	490	980	1010
Si	7480	10 720	7000	10 710	10 800

wt%	Colza	To	WL	To-WL	WL-To
C	41.2	46.9	44.0	47.6	50.1
H	6.01	5.77	6.38	5.98	6.02
N	0.51	0.54	0.3	0.36	0.34
O	44.1	41.0	45.0	42.2	41.5
S	0.33	0.36	0.1	0.1	0.11
mg kg^{-1}		Ash components (major elements only)			
Cl	8340	915	588	349	341
Al	31	20	20	40	20
Ca	8430	8920	4730	4760	6284
Fe	7	7	7	18	7
K	22 370	24 570	3147	3250	3990
Mg	552	662	227	253	304
Na	1199	1710	185	200	235
P	242	413	63	130	78
Si	98	47	30	70	30

wt%	Corn	To	WL	To-WL	WL-To
C	41.4	49.0	42.9	48.1	48.4
H	6.11	5.74	6.21	5.9	5.27
N	0.6	0.5	0.49	0.57	0.52
O	44.3	37.6	41.8	40.3	38.0
S	0.11	0.13	0.1	0.1	0.11
mg kg^{-1}		Ash components (major elements only)			
Cl	3434	989	228	273	310
Al	1010	610	1251	550	1215
Ca	6110	3270	3070	3110	4209
Fe	686	224	758	270	574
K	11 400	25 000	5970	4470	9070
Mg	2800	2480	1652	1740	2033
Na	86	196	155	100	147
P	940	1293	700	573	909
Si	17 100	10 130	21 200	10 800	19 210

leaching also has a correspondingly positive effect on the K content, since it is removed with the washing water. Moreover, sulfur and phosphorus could be removed partly due to different solubility of several sulfur or phosphorus compounds. Samples have been washed twice, and the effect on decreasing the Cl content becomes clearer when the first and the second washing cycles are compared against one another (Fig. 2).

A significant decrease of chloride in the washing water is observed after the second washing cycle. Regarding the torrefied samples, especially corn straw, the chloride content after the first washing cycle appears to be lower in contrast to the source material. Torrefaction generally improves the hydrophobic characteristics of the samples.[42] Due to hydrophobic surfaces of the determined feedstock material, inorganic compounds respectively salts could be more effectively removed through water-leaching.

In addition to the ultimate analysis, the ash content provides further information on different effects of the applied pre-treatment methods. The ash content for each sample was determined gravimetrically (550 °C, 36 h) and is displayed in Fig. 3.

Basically, leached samples provide the lowest ash content compared to the raw or the torrefied materials (as well as the pre-washed and post-washed ones). Conversely, this means that a higher content of inorganic species was removed with the washing water. The torrefied fuels (barley and wheat) show a slightly elevated ash content, which may be explained by the increased density of the sample materials. Colza straw shows a significantly higher chloride content (Table 1), and torrefaction pre-treatment seems to reduce the ash content by about one weight percent. Shang et al.[43] have reported that methyl chloride has been detected in the volatile torrefaction products, however, the effect of this thermal process on biomass chlorine content has not been studied commonly. The density
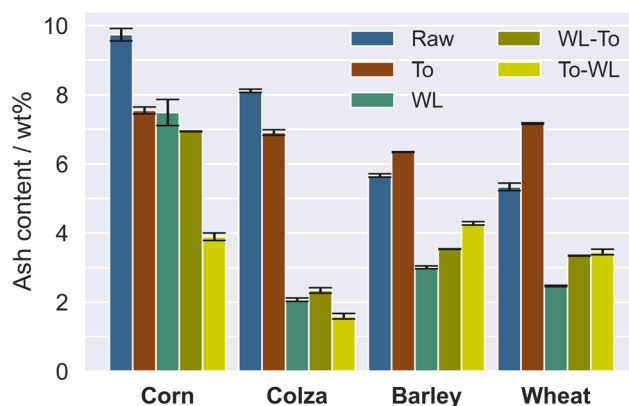

Fig. 3 Amount of ash depending on different pre-processing methods. The ash contents are presented on a dry solid basis.

of both WL-To and To-WL materials increased slightly in comparison with biomass which has only been leached, but is nonetheless clearly lower than the torrefied material.

For both barley and wheat straw ash, the proportion of inorganic components is found to be higher in To-WL than in WL-To. This supports the hypothesis that the release of chlorine by torrefaction treatment might reduce the water solubility of the ash components, and therefore, the inorganic content increases. In a study published elsewhere,[44] results revealed that subjecting biomass to torrefaction treatment improved its hydrophobic properties. The water-soluble elements leached from biomass are mainly Cl, S, N, P, K, Na, Mg, and Mn,[45] whereby especially herbaceous types exhibit generally a high proportion of chlorine.[7] Thereby, the most mobile water-soluble phases in biomass include K-, Na-, Ca-, Mg-, and Fe-bearing minerals among chlorides, nitrates, sulfates, carbonates, and oxalates.[45]

3.1.2 Release of inorganic constituents. The pre-treated samples listed in Table 1 have been investigated by MBMS in order to elucidate the release behavior and fate of inorganics. Both devolatilization and char gasification/ash reaction stages were examined. A semi-quantitative analysis was performed, which allows the determination of relative peak intensities, thus clarifying the influence of different applied pre-treatment methods. This improves a comparison of the generated data among themselves, however, an absolute conclusion about the species (i.e., absolute concentration of species such as KCl, SO2, and so forth) content cannot be drawn. Fig. 4 shows a general overview of recorded mass spectra for pre-treated wheat straw. The signal-intensity profiles exemplify the effect of the applied treatment as a representative example for KCl (m/z 74).

A short volatile peak can be observed at the very beginning of the measurement, which represents the devolatilization/pyrolysis peak, whereas in the second step, a significantly broader peak occurs, and this signal belongs to the release of matter which is stronger chemically bound. Thus, the signal denotes the occurrence of the char gasification and ash reactions, which appear typically after the pyrolysis process. The pyrolysis peak is characteristically denoted by a fast reaction
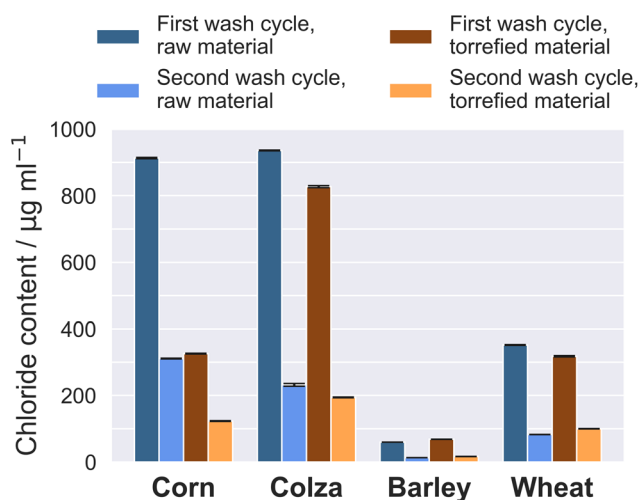

Fig. 2 Comparison of the chloride content detected in the washing water after the first and second washing cycle (for raw and torrefied straw samples).
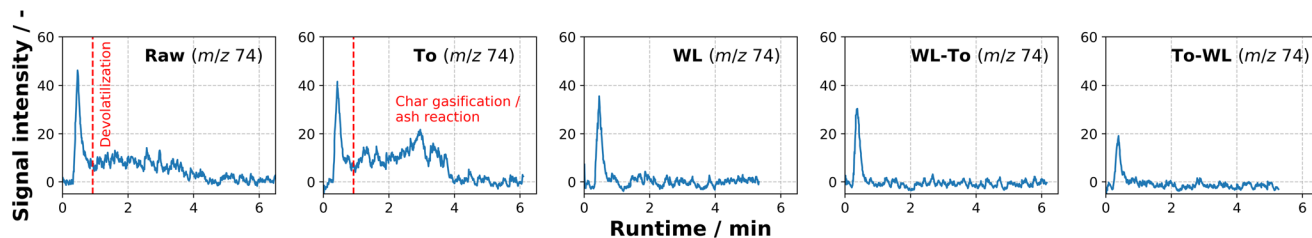
Fig. 4 Intensity-time profiles of KCl$^+$ (*m/z* 74) depending on different pre-treatment methods. The intensity-time profiles exemplify the effect of the applied pre-treatments. Both WL-To and To-WL show almost no more release during char gasification/ash reaction. The peak areas are proportional to the amount of species released.

kinetic, whereas the char gasification and the ash reaction are denoted by a slow kinetic rate. For example, potassium releases to the gas phase in two steps. First, organically bond potassium (note the biomass constituents lignin, cellulose and hemicellulose) is released in a low-temperature range of up to 500 °C. This stage is understood as the devolatilization and is insensitive to the chlorine content in the fuel. In the second step, following temperatures above 500 °C, potassium releases at full speed mostly in form of KCl and KOH, depending on the chlorine content.

In Fig. 5, the normalized results of different peak areas are presented in form of bar diagrams (for both devolatilization and char gasification/ash reaction). Three measurements per sample were taken and the results were averaged. Only masses with a signal well above the background signal were further evaluated. The results of the semi-quantitative analysis were generally in good accordance with the results of the chemical characterization (Table 1). In contrast to the source materials, the torrefied samples show a lower amount of chlorine released. The water-leached samples show obviously clearer effects on the release behavior; particularly the amount of released Cl, HCl and K is significantly reduced. The release of sulfur-containing compounds (H$_2$S, SO$_2$ and COS) also tends to be slightly reduced. The partially scattered range of the error bars indicates an inhomogeneous distribution, and this can be explained by the fact that biomass typically exhibits fibrous, heterogeneous properties.[46]

Both raw as well as torrefied samples show primarily secondary releases in form of char gasification or ash reactions (note the lower bar charts in Fig. 5). Predominantly, some amounts of K, SO$_2$ and partly Cl are released due to less volatile compounds in the ash. During this reaction part, species are released which are less or without reaction partner not volatile in contrast to the devolatilization part. For example, sulfur is released in form of sulfur dioxide from stronger bound organic compounds or sulfates. Most likely, organic sulfur, which is stronger bound was released before inorganic sulfur compounds are released. An additional crucial observation is that the water-leached samples show virtually no more secondary release for almost every inorganic compound.

For direct comparison, the partly large differences in the sample composition and the effect of the pre-treatment methods on different fuels is highlighted in Fig. 6. The corre-
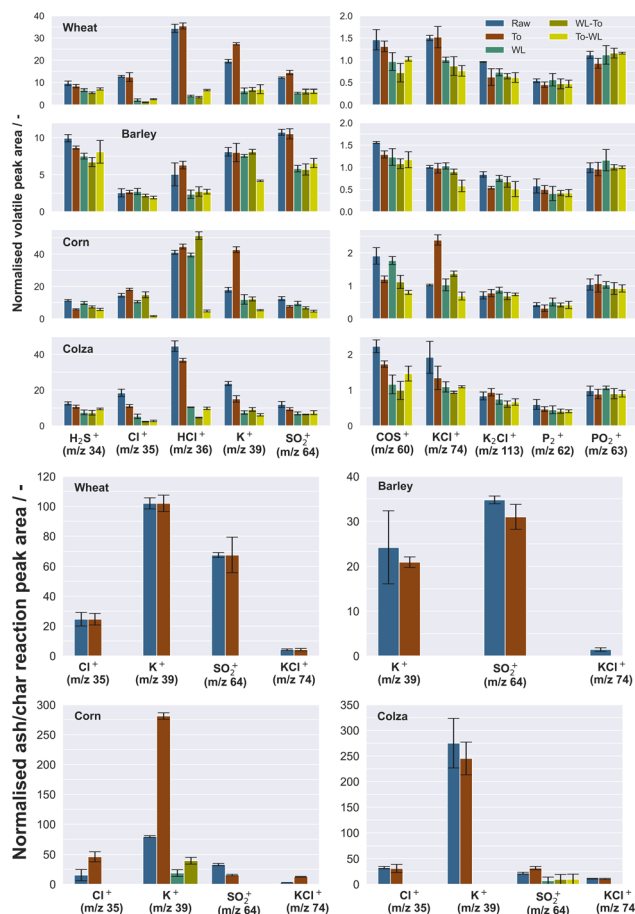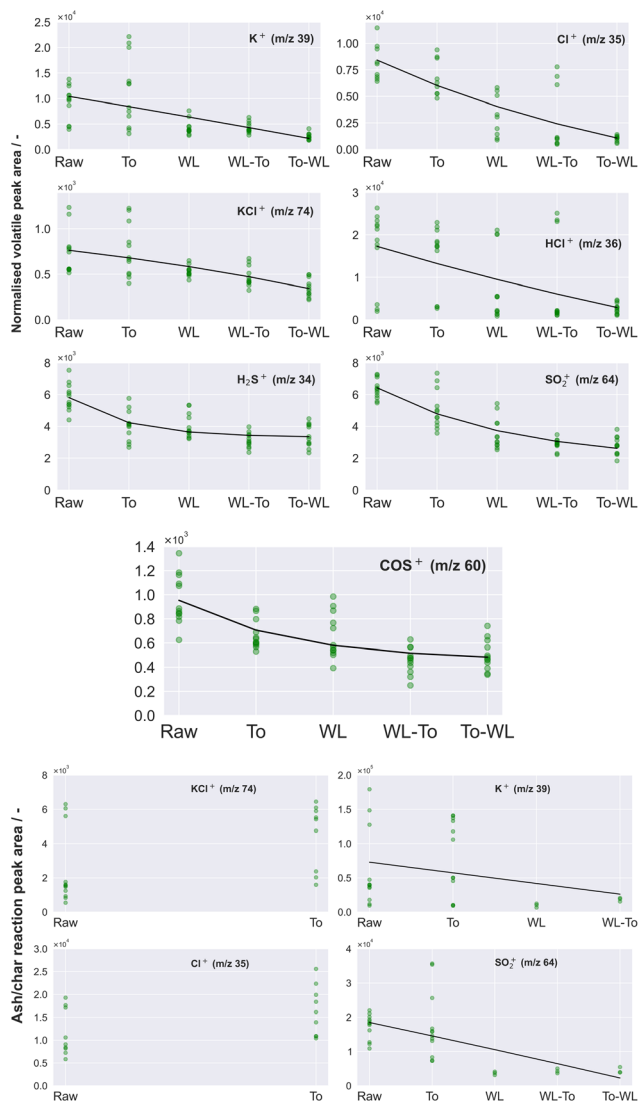

Fig. 5 Averaged, normalized peak areas of species released during pyrolysis/devolatilization phase (top) and char gasification or ash reactions (bottom).

lation between the normalized volatile peak area of problematic species and the pre-treated samples are summarized. The scatter plots clarify a certain trend between the pre-treatment methods and the released amount of volatile species. Samples, which were first torrefied and then washed afterwards (To-WL) tend to show the strongest effects in terms of reducing the amount of problematic, volatile species. Moreover, the scatter plots emphasize a relatively inhomogeneous composition of the fuel samples altogether.

Fig. 6 Summarized correlation between the normalized volatile (top) and char gasification/ash reaction (bottom) peak area of K, Cl, KCl, HCl, H_2S, SO_2, COS and the pre-treated materials (corn, colza, barley and wheat straw).

Likewise, for the secondary ash reactions, the scatter plots are exhibiting the correlation between the normalized char gasification/ash reaction peak area (lower scatter plot in Fig. 6) of detected inorganic species and the applied pre-treatment methods. For both KCl and Cl, no more release is observed in case the samples were prewashed before. Due to a higher material density, the torrefied samples tend to show a larger amount of released Cl and KCl as well. A significant decrease in K or SO_2 for washed samples is also observed for the secondary reaction part.
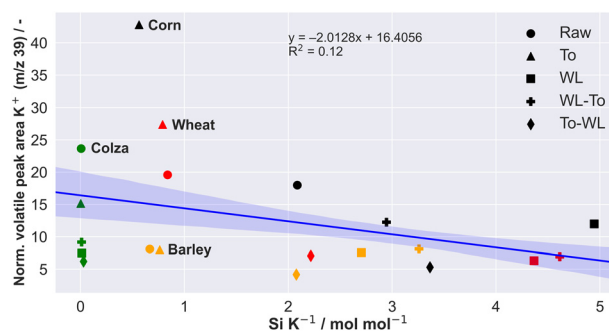
According to previous studies published elsewhere,[47–49] it has been reported that the molar Si/K ratio might be representative as an indicator for the potassium release in the gas phase: a high molar Si/K ratio corresponds or leads to a preferred formation of potassium silicates, which are bound in the bottom

ash. Previous studies well documented that alkali metal oxides may be chemically incorporated into silicate networks and thus become less volatile.[50–52] In Fig. 7, data regarding the correlation between the molar Si/K ratio and the K release, gained from the batch-type release experiments (Fig. 5) are presented. A clear correlation between the molar ratio of Si/K and the release behavior of K could be observed. The release of K tends to decrease with a constantly increasing molar Si/K ratio.

Fig. 7 implies that a higher concentration of Si in relation to K limits the gas phase activity of K. Moreover, the results highlight the effects of the applied pre-processing methods. While the raw material as well as the torrefied samples are associated with a higher release activity of potassium, the water-leached samples seem to prove quite the opposite. A decrease in K in the sample material shifts the ratio towards Si and this means a corresponding decrease in K release. Sommersacher et al.[53] reported that other parameters, such as the fuel bed temperature as well as the association of K in the fuel, seem to have a strong influence on the K release.

3.1.3 Mineral composition of ashes. Sample ashes produced in a gasification-like atmosphere were investigated diffractometrically by XRD in order to understand the crystalline phase formation of inorganic species and the interactions between them as well. The detected mineral phases are listed in Table 2. Since a quantification of identified crystalline phases and amorphous or unknown phases were only possible by adding an internal standard, the approximate ratios of the crystalline phases were determined.

In spite of relatively high measurement inaccuracies, major trends are presented, which provide general indications. The relative error of quantification was estimated at about 20 wt%. Basically, the diffractometric analyses show that ash samples contained considerable proportions of amorphous phases (generally found to be the major component of the ash samples). This made the detection of crystalline phases rather difficult. Therefore, not every individual determined Bragg reflection peak could be assigned to a crystalline phase. E.g., the identification of the phase $K_{9.6}Ca_{1.2}Si_{12}O_{30}$ in barley straw ash or illite in corn straw ash should be considered as questionable or rather as a suggestion for a possible mineral phase. Nonetheless, illite supported the assumption that corn straw is

Fig. 7 Molar Si/K ratio versus K release during devolatilization for the pre-treated herbaceous fuels. The confidence interval is set at 68%.

Table 2 Overview of the most important mineral phases (detected by XRD) found to be stable under gasification-like conditions. Due to a relatively high measurement inaccuracy, rough orientation values are presented: <10 wt% (−), 10 wt% to 30 wt% (+), 30 wt% to 50 wt% (++), and >50 wt% (+++)

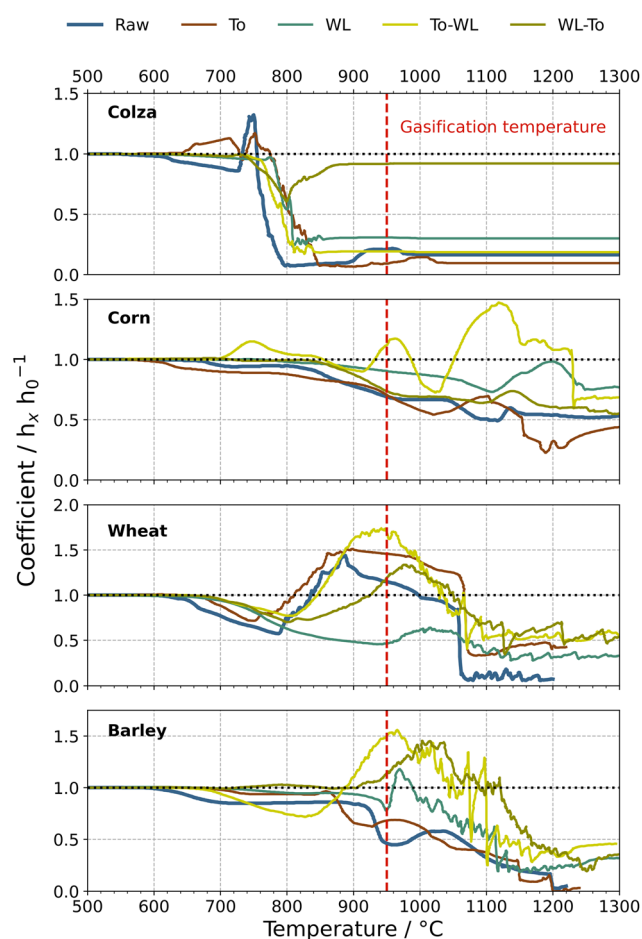| Phase	Feedstock	Raw	To	WL	WL-To	To-WL
KCl (Sylvite)	Wheat	++	++			
	Barley	−	−			
	Corn	+	+++	−	−	
	Colza	+	+			
K_2SO_4 (Arcanite)	Wheat	+++	+++			
	Barley	+	++			
	Corn					
	Colza	+	+	−	−	−
$K_2CO_3(H_2O)_{1.5}$	Wheat	+				
	Barley	+	+			
	Corn					
	Colza					
$CaCO_3$ (Calcite)	Wheat					
	Barley	−	−	+++	+++	+++
	Corn	−		−	−	+
	Colza	+	+	+++	+++	+++
$K_2Ca(CO_3)_2$ (Fairchildite)	Wheat					
	Barley	−	−			
	Corn					
	Colza	++	++	++	+	++
$K_{9.6}Ca_{1.2}Si_{12}O_{30}$	Wheat					
	Barley	+	+			
	Corn					
	Colza					
SiO_2 (Quartz)	Wheat					
	Barley					
	Corn	++	−	+++	+++	+++
	Colza					
$KAl_4Si_2O_9(OH)_3$ (Illite)	Wheat					
	Barley					
	Corn	+		+	+	+
	Colza					
$Ca(OH)_2$ (Portlandite)	Wheat					
	Barley					
	Corn					
	Colza			+	−	

obviously contaminated with soil impurities. Note that illite is considered a common clay mineral/layered silicate, and in combination with quartz, the probability that the straw sample investigated is contaminated with soil material is quite high.

Major phases found in raw biomasses are typically KCl, SiO_2, carbonates (mainly in form of $CaCO_3$), sulfates (mainly in form of K_2SO_4), and phosphates,[54,55] which were also found for the feedstocks under investigation. Each sample series contains more or less significant amounts of KCl, which is mainly reduced by washing the fuel itself. The results correspond well with the results of the ultimate analyses. Neither washing nor thermal treatment affects silica-based phases directly. However, both washing and torrefaction increase the density of the materials, which in turn effect a shift of certain inorganic proportion, e.g. SiO_2. The mineral phase proportions obtained by XRD investigations are also in good agreement with the ultimate analyses listed in Table 1.

Note that the formation of crystalline phases strongly depends on the ashing temperature. Some phases will form with increasing temperature (e.g. silicates or aluminosilicates), whereas other phases will decompose, e.g. chlorides or carbonates.[56] Likewise, it was reported that the heating rate might exert a significant impact on the thermal characteristics of ash samples; Yang et al.[57] have found that different heating rates showed a significant effect on fusion characteristics.

3.1.4 Ash fusion behavior. Ash samples were investigated by hot stage microscopy (HSM) in order to elucidate findings on ash fusion characteristics. In Fig. 8, the determined height profile coefficients h_x/h_0 of treated straw ashes are plotted depending on the temperature. It can be observed that each biomass variety appeared to have its own characteristic profile. Based on their profile changes h_x/h_0, it becomes clear that biomass-based ashes show rarely the same properties as already reported in DIN 51730 ("Testing of solid fuels – Determination of fusibility of fuel ash"), which is explained due to inhomogeneity of the samples. Generally, it can be said that the fusion process of biomass ash includes moisture evaporation, oxidation of organic matters and removal as well as reaction of inorganic matters at elevated temperature.[58]

Fig. 8 Height profile (coefficient h_x/h_0) of ashes investigated by HSM depending on increasing temperature for pre-treated colza, corn, wheat and barley straw ash. The dashed red line denotes the defined gasification temperature of 950 °C.

Typically, the coefficient h_x/h_0 exhibits a slight decrease beginning at low temperature ranges (600 °C to 700 °C). Besides sintering, shrinking in this temperature range may be explained by reaction of carbon contained in ash with CO_2 in the atmosphere, since the ash produced in a gasification-like environment exhibited a relatively high amount of residual carbon. The ash content of the fuel samples (assuming that the samples were completely combusted) was generally in a range between 5 wt% to 10 wt% (Fig. 3). In contrast, the amount of ash, prepared under gasification-like conditions, resulted typically in a range between 12 wt% to 19 wt%, which indicates a noticeably increased residual carbon content in the ash. A blackish shade of the ash samples was observed, and this also indicated that the organic matter was not completely converted. Independent from the applied pre-treatment methods, colza straw ash shows a noticeable low melting temperature, indicated by the steep decrease of the coefficient h_x/h_0, whereas corn and barley straw ash start to melt at higher temperatures. In general, ash samples are either completely molten or swelled from a temperature range of 950 °C. Nonetheless, slight tendencies can be seen, *e.g.* water-leached samples seem to start melting at higher temperatures in contrast to the raw or torrefied fuel ashes. Although untreated colza straw ash already shows a change of the coefficient h_x/h_0 at 600 °C, a noticeably change is observed for the washed sample at a temperature above 750 °C. This in turn means that reactions with ash components might be shifted to higher temperature ranges. The effect becomes clearer when comparing sample photos of both raw and water-leached samples under the same temperature conditions. Fig. 9 highlights the effect of water-leaching exemplary on the basis of colza straw ash.

First noticeable changes regarding the geometry of the cylindrical samples are observed at temperatures above 800 °C, which is in an appropriate accordance with the melting points of both alkali chlorides (KCl = 771 °C and NaCl = 802 °C). Interestingly, the coefficient h_x/h_0 of the water-leached colza remains constant in contrast to both raw and torrefied materials. Washing samples removes water-soluble elements, such as alkali chlorides from the biomass, which consequently improves the biomass fuel characteristics at elevated temperatures. For most of the sample ashes, volume increase starts at around 1000 °C, which might result from thermal decomposition of certain species (most likely potassium sulfate, since it

was detected in ash samples *via* XRD investigations, see section 3.1.3.).

In summary, washing pre-treatment has proven to influence the ash fusion behavior by means of removing alkali chlorides, but nonetheless, the effect was not sufficient for an appropriate operation at a gasification temperature of 950 °C. Torrefaction solely is not effective enough for removing problematic species, such as alkalis, and therefore, the ash fusion behavior is not affected positively in form of an increased ash melting point. In a recent investigation,[34] we provided causal evidence for $CaCO_3$-blended wheat straw, where most promising results regarding ash fusion characteristics were achieved. Investigations have shown that for samples including Ca-based additives, the ash melting point could be increased significantly due to interactions with silicate compounds and thus lowering of eutectic effects.[12]

3.2. Thermodynamic modelling

3.2.1 Condensation of volatile inorganics. Numerical predictions on condensation behavior of inorganic compounds (alkali chlorides, carbonates, sulfides and slag-mixtures), starting from 950 °C were performed for the pre-treated samples. Firstly, the release of inorganics (950 °C, 1.013 bar) was calculated and the resulting gas phase was deployed as input for the condensation computations (in a range from 950 °C to 400 °C, 1.013 bar).

Although the amount of condensed alkali chlorides (KCl/NaCl) hardly exhibited any differences between pyrolysis and char gasification/ash reaction, carbonates, sulfides and slag-mixtures show slight differences. The calculated amounts of condensed alkali chlorides are shown in Fig. 10.

Regarding the source materials or the torrefied samples, the condensation temperatures of both alkali chlorides are close to or above the melting points of KCl or NaCl. Water-leaching, regardless whether combined with torrefaction treatment beforehand or afterwards shifted the condensation temperature to lower range. In addition, a crucial outcome of the calculations is a sharp decline in amount of condensed alkali chlorides. The washed samples show the strongest effect in terms of lowering the amount of condensed alkali salts. However, torrefaction pre-treatment of the samples after or
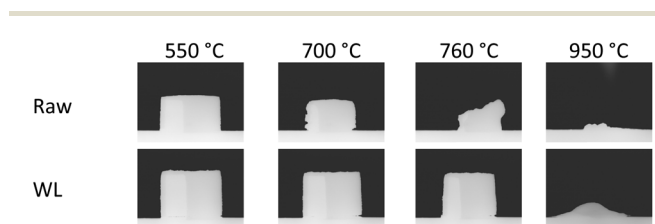
Fig. 9 Photos taken during ash fusion test for colza straw ash. In comparison with the source material, the change of the pellet geometry clarified the water-leaching effect on the ash melting behavior distinctly.
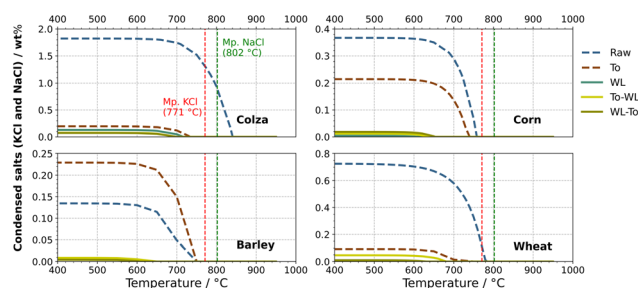
Fig. 10 Condensation of alkali chlorides (mostly potassium chloride) under gasification conditions. Both, red and green dashed lines denote the corresponding melting temperatures of KCl and NaCl. The gasification temperature is 950 °C.

before washing shows no further differences regarding the condensed amount of chlorides below 950 °C. Interestingly, torrefied barley straw exhibits a slightly increased proportion of condensed alkali chlorides in comparison to the raw material itself. Usually, the opposite case is observed or expected, when comparing with the other straw varieties. According to the chemical characterization (Table 1), an increased proportion of chlorine is detected in the torrefied barley straw in contrast to the source material. The presence of chlorine is indispensable for the formation of KCl, and this connection may explain an increased condensation activity of the torrefied material.

In addition to the alkali chlorides, other types of salt were found to condense. Fig. 11 exhibits the formation of condensed carbonates and slag-mixtures, predicted for gasification conditions.

According to thermodynamic equilibrium predictions, colza straw shows significant amounts of condensed carbonates or slag-mixtures for each sample pre-treated beforehand, regardless of the method applied, and the highest activity of all straw types investigated. The slag consists mainly of molten carbonates (K_2CO_3 and small proportions of $CaCO_3$ as well). Below 900 °C, the slag gradually transforms into solid carbonates. The chemical characterization has shown that colza has a conspicuously low silicon content (Table 1). This means that both calcium and potassium must react with other elements instead of silicon. As already observed for the condensed amount of alkali chlorides, torrefied barley straw shows a higher proportion of condensed species in contrast to the source material itself. Except for colza straw, all straw types if washed beforehand, show no more activity regarding condensed carbonates or slag-mixtures. A smooth phase transition between the slag and the carbonates is observed for colza straw.

3.2.2 Mineral phase transformations of ashes. The proportions of mineral phases depending on the process temperature were predicted for both pyrolysis and gasification-like conditions. No significant differences were observed between both conditions. Therefore, the focus in the following will be on gasification. Firstly, all phase compounds were numerically predicted depending on the process temperature, starting from 400 °C and ending at 1300 °C. The main phases were
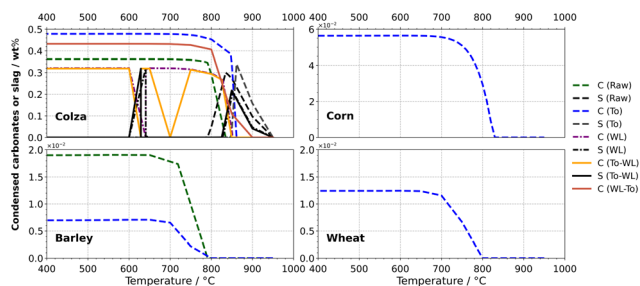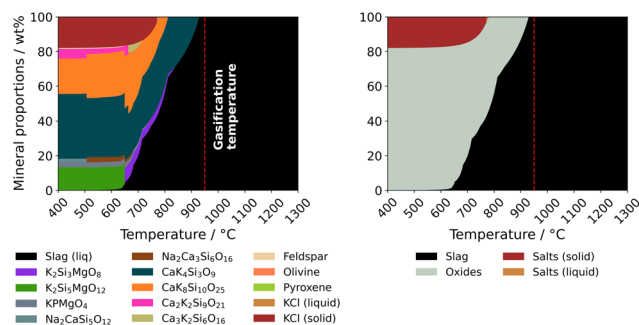

Fig. 12 Calculated mineral compositions of raw wheat straw ash under gasification-like conditions. An overview phase map is exemplarily presented, where all predicted phases are mapped (left), and summarized phases, mainly consisting of oxides, molten slag, solid or molten alkali metal chlorides and partially carbonates (right). The dashed red line denotes the gasification temperature of 950 °C.

summarized and sorted for a better overview (solid or molten alkali chlorides, carbonates, oxides/silicates and molten slag). Fig. 12 exemplifies the computed phase composition as a representative example for raw wheat straw ash, in which the complete phases as well as the grouped phases are displayed.

The complete overview of the calculated mineral proportions for each pre-treated feedstock is mapped in Fig. 13. Mixed carbonate compounds, mainly containing K and Ca belong to carbonates, and numerous silicates as well as other (mixed) oxides belong to oxides. The alkali salts consisted mainly of KCl, but small traces of NaCl may also be present (with regard to the solid as well as liquid phase compositions). As expected, the torrefied and the water-leached samples show a noticeably lower alkali chloride content than the source
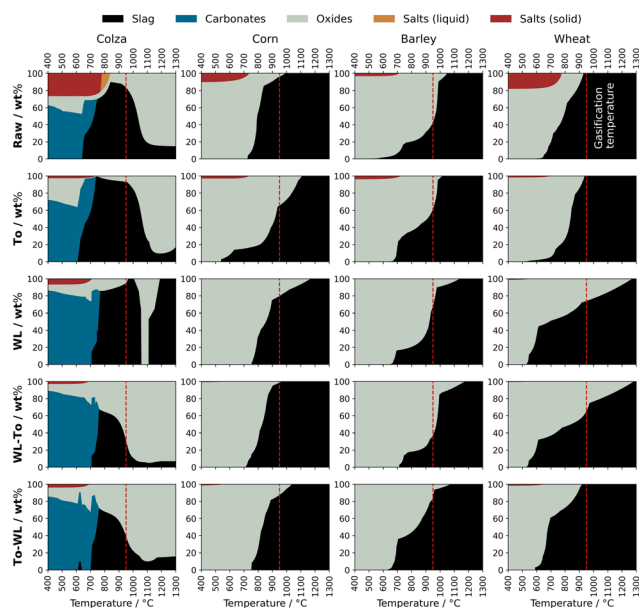

Fig. 11 Calculated condensation of carbonates (C) and slag mixtures (S) under gasification conditions. The gasification temperature is 950 °C.

Fig. 13 Calculated mineral proportions for pre-treated straw ash varieties in gasification-like environment. The dashed line denotes the fixed gasification temperature (950 °C).
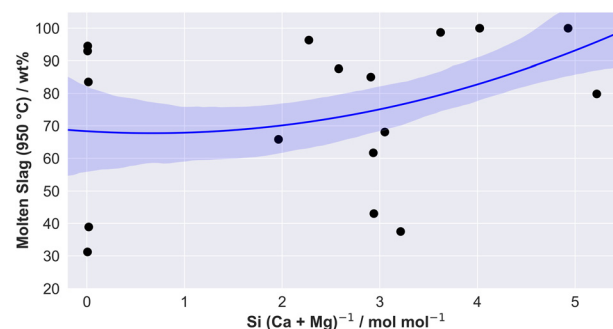
material, which is due to a significantly lower Cl content in the treated fuel. Independent of the applied pre-treatment methods, colza straw ash forms a significantly high proportion of carbonates in the low temperature range (between 400 °C and approximately 750 °C). In the temperature range above 800 °C, carbonate formation could no longer be observed, since $CaCO_3$ decomposed thermally or various reactions or melting processes were induced by potassium containing carbonates. Calcite decomposes to CaO and CO_2 at temperatures above 600 °C.[59]

The thermodynamic modelling results for colza straw ash show that at temperatures above 900 °C a noticeable high proportion of CaO as main oxide component is present. The slag partially contained carbonates, which clarifies or explains the direct, fluent phase transition from carbonate to slag. Moreover, the formation of solid oxides or silicates between 1050 °C and 1100 °C (notice the solid phase range between slag) is particularly conspicuous for the water-leached sample. In this range, Ca_2SiO_4 shows a significantly increased thermodynamic stability. This means that calcium-rich phases formed and thus, high-melting calcium silicates were generated, which did not occur in the slag due to their relatively high melting point. Likewise, in addition to carbonate compounds, untreated colza straw ash exhibits in the low-temperature range a high proportion of about 20 wt% of alkali chlorides, consisting mainly of KCl. From about 770 °C, the alkali salts transform into a liquid phase. The phase transformation coincides well with the melting point of KCl (773 °C).

Taking a closer look at the predicted phase formations of wheat straw ash, it becomes clear that washing exerts a conspicuous effect on the ash melting behavior. While the raw material itself shows 100 wt% of molten slag at 950 °C, the water-leached sample shows almost 70 wt% instead. Likewise, a significant fraction of KCl is washed out, which explains the higher proportion of solid oxides at 950 °C. Water-leaching treatment before torrefaction (WL-To) seems to be more promising than *vice versa*: at 950 °C, approximately 60 wt% of the ash is molten, whereas the torrefied/water-leached (To-WL) ash shows almost 100 wt% molten slag under the same conditions. However, this effect seems to be exactly reversed in the case of barley straw ash. In contrast, corn and colza straw ash, regardless of whether the samples were first washed and then torrefied or *vice versa*, did not show any decisive effects regarding their ash melting behavior.

At this point, however, it should be emphasized that the thermodynamic calculations are describing ideal equilibrium conditions and may deviate from real melting processes due to kinetic influences.

The molar ratio of Si/(Ca + Mg) is a suitable indicator for providing first information about ash-melting tendencies in systems dominated by Si, Ca, Mg, and K. Thereby, a decreasing melting temperature correlates with an increasing molar ratio.[53] It has been reported that the molar Si/(Ca + Mg) ratio allows for predicting the slagging tendency for residential heating appliances, where with rising value, slagging increases.[60] Fig. 14 shows a correlation between the molar ratio Si/(Ca + Mg)

Fig. 14 Molar Si/(Ca + Mg) ratio *versus* calculated amount of molten slag (100 wt%) for the pre-treated herbaceous fuels. The slag amount for each sample correspond to the predicted results presented in Fig. 13 at 950 °C. The confidence interval is set at 68%.

versus the predicted amount of molten slag formed at 950 °C for the summarized, pre-treated straw varieties (according to the determined slag proportions in Fig. 13). The previously mentioned correlation between the molar ratio of Si/(Ca + Mg) and the ash-melting behavior tend to underline the hypothesis. The higher the proportion of Si in relation to Ca and Mg, the higher the proportion of slag being formed and, consequently the lower the melting point of the ash.

Fig. 15 compares the ash fusibility of the pre-treated straw varieties in ternary phase diagrams (taking into account the main ash forming components CaO–K_2O–SiO_2).

Besides CaO and K_2O, small amounts of MgO and Na_2O were detected in the samples, which were considered for the normalization (mathematically added to CaO respectively K_2O) due to their similar chemical properties. Almost all ash samples, regardless of their pre-treatment, are located in the two-phase-region (solid–liquid). Interestingly, the SiO_2 content in colza straw ash, for example, is relatively low, whereas K_2O is the dominant key component. This means that high-melting calcium silicates cannot be formed. A possible approach would be to combine water-leaching and/or Ca addition and a supplementary SiO_2 addition in order to reach the solid phase area (notice both arrows, indicating the desired phase transition in Fig. 15, top left). Due to the shift in the ash composition (K_2O–CaO), washed samples would require a significantly lower SiO_2 content in contrast to the raw material itself.

Summarizing the central statement, it can be said that predicted phase diagrams indicated here that the applied pre-treatment methods provide distinct effects for increasing the amount of solid phases at 950 °C, nonetheless, further (combined) approaches are needed in order to increase the solid fraction, *e.g.* Ca- or Si-based additives or appropriate biomass blends.

4. Discussion

In the present study, the influence of different biomass upgrading technologies, such as torrefaction, water-leaching or combination of both steps on behavior of inorganic constituents was investigated in detail by means of experimental
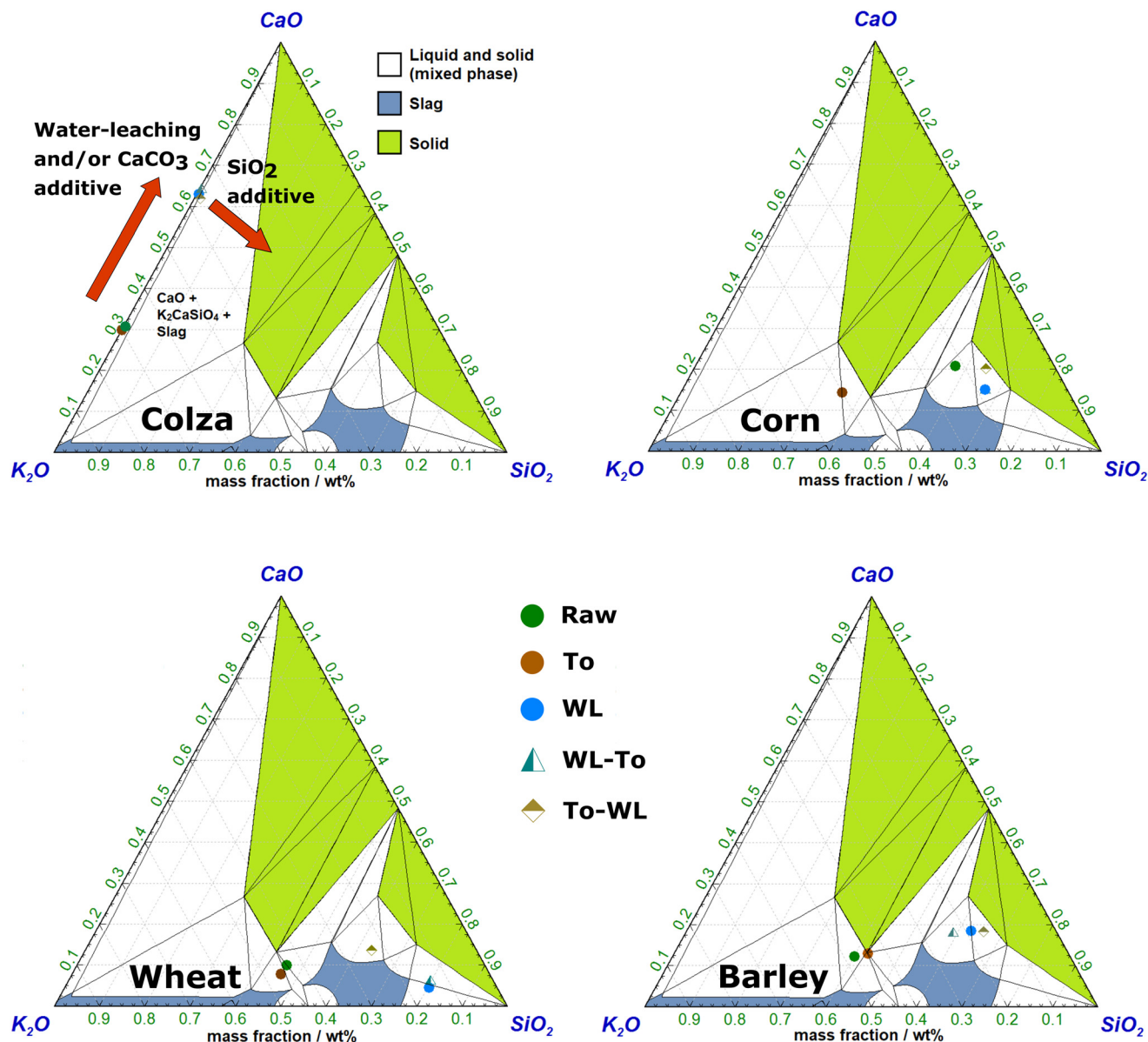
Fig. 15 Ternary phase diagrams for the SiO_2–CaO–K_2O system using FactSage.[61] The phases were predicted for (pre-treated) colza, corn, wheat and barley straw. The calculations were performed under isothermal/isobaric conditions at 950 °C and 1.013 bar.

methods and numerical approaches. Additionally, samples have been washed twice whilst taking into account the same quantity of washing water, and for two hours instead of conventional approaches (*e.g.* 24 h in total).

Regarding the impact on BCLG, subsequent inferences can be stated: the ultimate analysis has shown that different straw varieties reveal significant differences or inhomogeneity in terms of their inorganic composition. This became also clearly visible in the scatter plot diagrams (Fig. 6). Thereby, the results showed clear differences regarding the composition of various biomass feedstocks investigated. Thus, it becomes obvious that a wide range of fuels should be investigated in order to draw conclusions about the inorganic composition and the corresponding impact on ash-induced problems.

According to thermodynamic calculations and XRD investigations, colza straw ash, for example, shows an intensive formation of carbonates, whereas the other straw ashes did not show this effect to the same extent. At temperatures above 900 °C, there were practically no more carbonates formed, regardless of the sample composition. In practice, this means that at high gasification chamber temperatures and short ash residence times, low carbonate contents might be expected in the ash produced, similar to those conditions in a combustive environment.[62] Conversely, this means that Ca is thus predominantly present as burnt lime in the ash. Torrefied samples have shown in general an increased amount of ash, whereas the opposite was observed for the water-leached samples. It is found that torrefaction is an effective method to reduce the

chlorine content in the fuel significantly,[63] which in turn should minimize the risk of high-temperature corrosion in the gasifier. However, the alkali content remained steady or was even increased by torrefaction. As a consequence, unfavorable risk increases in terms of bed agglomeration, fouling and slagging are expected. Both, results obtained by HSM and predicted ternary phase diagrams proved that water-leaching has a positive effect on the ash melting behavior. In contrast to the raw or torrefied samples, the washed fuels showed a slightly increased ash softening point. Nevertheless, these pre-treatment methods were not effective enough in order to ensure a problem-free operation at 950 °C, as all ash samples have virtually melted completely at temperatures above 900 °C.

While most of the investigations have focussed on woody feedstocks so far, more studies on herbaceous feedstocks are essential.[64–68] Given the fact that herbaceous feedstocks are primarily associated with impurities, which are mainly ash-forming elements, makes them challenging for utilizing in thermal conversion processes. Woody biomass contains less problematic impurities, which cause difficulties, e.g. high-temperature corrosion, ash-deposit formation and air emissions (SO_x and NO_x).[69] Porbatzki et al.[70] found out that the amount of inorganic trace elements released from the herbaceous biomass was about one order of magnitude higher than from the woody biomass. Generally, woody biomass has a lower moisture content than herbaceous biomass. Several studies[71–73] reported on crucial advantages of woody biomass, when torrefied and combined with drying and densification, which turns it into a commodity fuel exhibiting enhanced energy density, hydrophobicity, grindability and homogeneity. In effect this means that upgraded woody biomass can be handled almost in the same way as coal and directly replace it.

On the downside, herbaceous feedstocks exhibit a lower calorific value, bulk density, ash melting point and higher content of ash impurities, which cause the aforementioned problems.[74] Those drawbacks can be relatively easily overcome by leaving straw residues on the field after harvesting. This has the advantage that rainfall can provide a natural leaching process and separates a large part of the sodium/potassium and chlorine. Alternatively, feedstocks can be directly washed by dedicated facilities at moderate temperatures or simply room temperature (20 °C). Link et al.[75] reported on the investigation of the effect of leaching treatment on the gasification of wine and vine (residue) biomass. It was found that leaching pre-processing impacted on the composition of the product gas and the tar content. The results indicated a lower tar yield (by 36%) and a higher yield of CO (by 17%) and H_2 (by 30%) and a higher LHV value (by 12%) as compared with the untreated source material itself.

It is important to note that the water waste streams generated for water-leaching pre-treatment should be taken into account for various resource recovery options. It has been demonstrated by Tobin et al.[76] that wastewater treatment plays an integral role in the operation of a biorefinery. Despite some difficulties such as capital costs, the evaporation of wastewater offers an operationally promising means to treating wastewater which incorporates various resource recovery options. In literature,[77] it was reported that specific biominerals such as struvite, a mineral which is rich in nitrogen, phosphorus and magnesium can be recovered and applied as a promising fertilizer. A variety of processes for the recovery of struvite from wastewater are applied, however, the costs of these processes cannot be well compared due to the differences in the operational conditions.[77] It is therefore definitely worthwhile to keep an eye on the wastewater approach and to promote appropriate processes in future studies.

In a previous study conducted by Gilbe et al.,[78] a correlation between the inorganic constituents and the ash fusibility was suggested: e.g., woody biomass fuels were considered and a "slagging index" was designed, where higher values of the molar Si/(Ca + Mg) ratios imply increased melt formation, and consequently higher risk for slag problem at a given temperature. Gilbe et al.[78] claimed that for wood derived fuels with a comparatively low inherent Si content, relatively moderate slagging tendencies were observed. It should be pointed out here that a severe contamination of sand (SiO_2) to (woody) fuels may greatly enhance adverse slagging tendencies. Similar observations were made with herbaceous feedstocks investigated in the present work, and the predicted amount of formed slag underlined a correlation depending on the molar Si/(Ca + Mg) ratio. According to thermodynamic equilibrium calculations, a lower molar ratio of Si/(Ca + Mg) has proven a positive trend in terms of lowering the molten slag formation. Water-leached samples have shown a significantly lower proportion of K_2O, which conversely leaded to a shift in the inorganic components present in the ash and increased the proportion of SiO_2 as well as CaO/MgO. The alkali metal content in biomass fuel has a major effect on slagging, since a high concentration of K in biomass fuel tends to favor the formation of low melting point compounds and thus, an increased slag formation.[12] Consequently, undesired interactions with the bed material or fouling in general are promoted accordingly. Since the ash characteristics of Si rich fuels were governed by silicate-alkali chemistry, thorough attention should be given to herbaceous feedstocks by upgrading them in terms of torrefaction and/or pre- or postwashing. The fact that chlorine and potassium are mostly bound as water-soluble KCl makes the treatment technologies previously discussed particularly promising.

Cl promotes the release of K in form of gaseous KCl significantly.[79] Therefore, the release of K depends upon the content of Cl in the fuels rather than on the potassium content. Condensed vapor-phases of alkali compounds generate deposits on the heat exchanger surface, which can cause severe fouling-related problems.[80] Hot gas analysis by MBMS confirmed that the proportion of alkali chlorides in the fuel was successfully reduced by water-leaching treatment. Due to the reduced amount of alkali chlorides released, their condensation in turn also shifted from temperatures above their melting point to temperatures below, so that fouling effects should be diminished. Besides Al and S, Si can trap alkali compounds before being deposited, thereby reducing the

alkali content released.[81] Batch-type release experiments have confirmed that the release behavior of potassium depended on the molar Si/K fuel ratio. A higher proportion of Si led to a reduced release of K, which should have a beneficial impact on fouling-related problems. Sommersacher *et al.*[53] have reported that for very high Si/K ratios (*i.e.*, for sewage sludge), a good embedding of K in the bottom ash and, consequently, a very low K release prevails.

The outcomes of the present work indicate that biomass upgrading has a major effect on the elemental composition of the feedstock, and consequently an impact on the behavior of inorganic constituents in BCLG. As discussed before, both, washing and torrefaction and especially their combination reduce the amount of elements known to cause or at least enhance ash related problems and thus improve the ash behavior. Note that this effect varies with the applied or combined pre-processing method as well as the biomass source. However, since the critical elements are not completely removed, it can hardly be predicted from the laboratory results, if ash related problems are solved or only reduced in full-scale application. Therefore, in a previous study,[34] we compared the characteristics pre-treated and additivated wheat straw to those of industrial wood pellets, which were selected as benchmark material on the basis of their low content of problematic inorganic constituents. The woody benchmark material showed promising outcomes in the sense of ash fusion behavior as well as the release and fate of problematic inorganics during gasification. It has been demonstrated in ash fusion testing, ternary SiO_2–CaO–K_2O phase diagrams, and in experimental hot gas analyses that the quality of the benchmark materials was almost reached when wheat straw was torrefied and/or pre- or postwashed. Among the straw varieties investigated in the present work, pre-traeted colza does by far not reach a quality similar to wood. Unfortunately, large scale tests with aforementioned fuels are still pending, so that further conclusions on the transferability of the laboratory results to application are not possible yet.

It can generally be concluded that both, experimental methods and thermodynamic modelling calculations have shown similar trends and the trends were logically comprehensible. The significance of the predictions was nonetheless partially limited, which may be caused by kinetic reasons and the non-equilibrium character of the experiments. Therefore, in addition to experimental investigations, an advanced numerical model including thermodynamics and kinetics of biomass gasification should be elaborated in future studies.

Both performance as well as economic impacts of pre-processed biofuels on final conversion stage were not assessed in this work, as an extensive techno-economic review is required in that case. However, many of those techno-economic analyses of key pre-treatment technologies have been discussed in the literature so far, *e.g.* in ref. 82–84. Abelha *et al.*[84] for example stated that for dry biomass, such as straw, postwashing of torrefied biomass is economically more attractive than prewashing, despite the fact that a slightly less effective removal of water-soluble inorganics like K and Cl may be expected. In addition, it was claimed that upgraded miscanthus (torrefied and postwashed), for example, can compete with conventional wood pellets in terms of fuel properties and prices in commercial and public sector buildings.

5. Conclusion

An in-depth survey throughout the present investigation was set on the influence of different (combined) pre-treatment measures on the behavior of inorganic constituents during gasification of herbaceous biomass. Thermal pre-treatment and/or water-leaching have been studied thoroughly and proven to change the ash chemistry noticeably and thus, affecting gasification and slagging characteristics. The following conclusions can be drawn:

• Promising results were achieved, when both torrefaction and water-leaching measures were combined with each other; torrefaction alone is suitable for decreasing the chlorine content, but not the amount of potassium as well.

• Washing feedstocks twice on a shorter timescale seems more favorable in terms of declining the content of chlorine. This means in turn a mutual benefit from the economic and ecological standpoint of saving costs, time and energy.

• The silicon content in the fuel ash promotes the formation of silicate networks and thus, leads to a preferred formation of potassium silicates. Conversely, the gas phase activity of potassium is decreased.

• According to thermodynamic modelling approaches, the ash fusion might be affected by the molar Si/(Ca + Mg) ratio. The higher the ratio, the higher the ash fusion temperature of the fuel ashes investigated.

• Herbaceous feedstocks show in general a relatively inhomogeneous composition regarding their ash constituents; therefore, the "thermal" stability and thus the ecological/economic effectivity should be increased by appropriate fuel blends. Thereby, machine learning methods may be promising approaches in order to provide fully understanding and optimization of the CLG process.

• It appears that postwashing of torrefied straw is economically more attractive than prewashing.

Author contributions

Florian Lebendig and Michael Müller conceived and designed the study. Florian Lebendig performed the experiments, the thermodynamic equilibrium calculations, the analysis and interpretation of the data, and wrote the manuscript. Michael Müller reviewed this paper and provided valuable suggestions. All authors read, edited, and approved the final manuscript.

Conflicts of interest

The authors declare no conflict of interest. The funders had no role in the design of the study; in the collection, analyses,

or interpretation of data; in the writing of the manuscript, or in the decision to publish the results.

Acknowledgements

References

1 L. M. Schaffer and T. Bernauer, *Energy policy*, 2014, **68**, 15–27.

2 J. Rogelj, A. Popp, K. V. Calvin, G. Luderer, J. Emmerling, D. Gernaat, S. Fujimori, J. Strefler, T. Hasegawa, G. Marangoni and others, *Nat. Clim. Change*, 2018, **8**, 325–332.

3 F. Cherubini, G. P. Peters, T. Berntsen, A. H. Strømman and E. Hertwich, *GCB Bioenergy*, 2011, **3**, 413–426.

4 V. S. Sikarwar, M. Zhao, P. Clough, J. Yao, X. Zhong, M. Z. Memon, N. Shah, E. J. Anthony and P. S. Fennell, *Energy Environ. Sci.*, 2016, **9**, 2939–2977.

5 U. Mohamed, Y. Zhao, Y. Huang, Y. Cui, L. Shi, C. Li, M. Pourkashanian, G. Wei, Q. Yi and W. Nimmo, *Energy*, 2020, **205**, 117904.

6 L. S. Nikolaisen and P. D. Jensen, *Biomass Combustion Science, Technology and Engineering*, 2013, 36–57.

7 A. Demirbaş, *Energy Explor. Exploit.*, 2003, **21**, 269–278.

8 H. J. Grabke, M. Spiegel and A. Zahs, *Mater. Res.*, 2004, **7**, 89–95.

9 E. Björkman and B. Strömberg, *Energy Fuels*, 1997, **11**, 1026–1032.

10 E. D. Lavric, A. A. Konnov and J. De Ruyck, *Biomass Bioenergy*, 2004, **26**, 115–145.

11 H. J. Pluim, M. Van Der Goot, K. Olie, J. W. Van Der Slikke and J. G. Koppe, *Chemosphere*, 1996, **33**, 1307–1315.

12 D. Boström, A. Grimm, C. Boman, E. Björnbom and M. Ohman, *Energy Fuels*, 2009, **23**, 5184–5190.

13 A. A. Tortosa-Masiá, F. Ahnert, H. Spliethoff, C. J. Loux and K. R. G. Hein, *Therm. Sci.*, 2005, **9**, 85–98.

14 A. Anukam, S. Mamphweli, P. Reddy, E. Meyer and O. Okoh, *Renewable Sustainable Energy Rev.*, 2016, **66**, 775–801.

15 K.-Y. Chiang, K.-L. Chien and C.-H. Lu, *Appl. Energy*, 2012, **100**, 164–171.

16 T. G. Bridgeman, J. M. Jones, I. Shield and P. T. Williams, *Fuel*, 2008, **87**, 844–856.

17 H. Chen, X. Chen, Z. Qiao and H. Liu, *Fuel*, 2016, **183**, 145–154.

18 H. P. Nielsen, F. J. Frandsen, K. Dam-Johansen and L. L. Baxter, *Prog. Energy Combust. Sci.*, 2000, **26**, 283–298.

19 J. M. Johansen, J. G. Jakobsen, F. J. Frandsen and P. Glarborg, *Energy Fuels*, 2011, **25**, 4961–4971.

20 S. B. Saleh, J. P. Flensborg, T. K. Shoulaifar, Z. Sárossy, B. B. Hansen, H. Egsgaard, N. DeMartini, P. A. Jensen, P. Glarborg and K. Dam-Johansen, *Energy Fuels*, 2014, **28**, 3738–3746.

21 Y. Niu, Y. Lv, Y. Lei, S. Liu, Y. Liang, D. Wang and others, *Renewable Sustainable Energy Rev.*, 2019, **115**, 109395.

22 W.-H. Chen, W.-Y. Cheng, K.-M. Lu and Y.-P. Huang, *Appl. Energy*, 2011, **88**, 3636–3644.

23 J. J. Chew and V. Doshi, *Renewable Sustainable Energy Rev.*, 2011, **15**, 4212–4222.

24 M. J. C. Van der Stelt, H. Gerhauser, J. H. A. Kiel and K. J. Ptasinski, *Biomass Bioenergy*, 2011, **35**, 3748–3762.

25 H. B. Tukey Jr., *Annu. Rev. Plant Physiol.*, 1970, **21**, 305–324.

26 K. Meesters, W. Elbersen, P. van der Hoogt and H. Hristov, *IEA Bioenergy*, 2018.

27 B. M. Jenkins, R. R. Bakker and J. B. Wei, *Biomass Bioenergy*, 1996, **10**, 177–200.

28 T. Garbowski, *Water, Air, Soil Pollut.*, 2019, **230**, 1–16.

29 X. Liu and X. T. Bi, *Fuel Process. Technol.*, 2011, **92**, 1273–1279.

30 T. Wigley, A. C. K. Yip and S. Pang, *Energy*, 2016, **109**, 481–494.

31 R. Tu, E. Jiang, S. Yan, X. Xu and S. Rao, *Bioresour. Technol.*, 2018, **264**, 78–89.

32 C. Yu, P. Thy, L. Wang, S. N. Anderson, J. S. VanderGheynst, S. K. Upadhyaya and B. M. Jenkins, *Fuel Process. Technol.*, 2014, **128**, 43–53.

33 A. Zheng, Z. Zhao, S. Chang, Z. Huang, K. Zhao, G. Wei, F. He and H. Li, *Bioresour. Technol.*, 2015, **176**, 15–22.

34 F. Lebendig, I. Funcia, R. Pérez-Vega and M. Müller, *Energies*, 2022, **15**, 3422.

35 M. Bläsing and M. Müller, *Combust. Flame*, 2010, **157**, 1374–1381.

36 M. Bläsing, M. Zini and M. Müller, *Energy Fuels*, 2013, **27**, 1439–1445.

37 C. H. Pang, B. Hewakandamby, T. Wu and E. Lester, *Fuel*, 2013, **103**, 454–466.

38 C. W. Bale, E. Bélisle, P. Chartrand, S. A. Decterov, G. Eriksson, A. E. Gheribi, K. Hack, I.-H. Jung, Y.-B. Kang, J. Melançon and others, *Calphad*, 2016, **55**, 1–19.

39 E. Yazhenskikh, T. Jantzen, K. Hack and M. Müller, *Rasplavy/Melts*, 2019, **2**, 116–124.

40 R. B. Bates and A. F. Ghoniem, *Bioresour. Technol.*, 2013, **134**, 331–340.

41 S. Ren, H. Lei, L. Wang, Q. Bu, S. Chen and J. Wu, *Biosyst. Eng.*, 2013, **116**, 420–426.

42 R. H. H. Ibrahim, L. I. Darvell, J. M. Jones and A. Williams, *J. Anal. Appl. Pyrolysis*, 2013, **103**, 21–30.

43 L. Shang, J. Ahrenfeldt, J. K. Holm, S. Barsberg, R.-Z. Zhang, Y.-H. Luo, H. Egsgaard and U. B. Henriksen, *J. Anal. Appl. Pyrolysis*, 2013, **100**, 145–152.

44 A. Dyjakon, T. Noszczyk and M. Smędzik, *Energies*, 2019, **12**, 4609.

45 S. V. Vassilev and C. G. Vassileva, *Energy Fuels*, 2019, **33**, 2763–2777.

46 M. J. C. Van der Stelt, H. Gerhauser, J. H. A. Kiel and K. J. Ptasinski, *Biomass Bioenergy*, 2011, **35**, 3748–3762.

47 J. N. Knudsen, P. A. Jensen and K. Dam-Johansen, *Energy Fuels*, 2004, **18**, 1385–1399.

48 A. Novakovic, S. C. van Lith, F. J. Frandsen, P. A. Jensen and L. B. Holgersen, *Energy Fuels*, 2009, **23**, 3423–3428.

49 M. Müller, K.-J. Wolf, A. Smeda and K. Hilpert, *Energy Fuels*, 2006, **20**, 1444–1449.

50 L. L. Baxter, T. R. Miles, T. R. Miles Jr., B. M. Jenkins, T. Milne, D. Dayton, R. W. Bryers and L. L. Oden, *Fuel Process. Technol.*, 1998, **54**, 47–78.

51 B. Sander, N. Henriksen, O. H. Larsen, A. Skriver, C. Ramsgaard-Nielsen, J. N. Jensen, K. Stærkind, H. Livbjerg, M. Thellefsen, K. Dam-Johansen and others, 1st World Conference and Exhibition on Biomass for Energy and Industry, 2000.

52 P. A. Jensen, F. J. Frandsen, K. Dam-Johansen and B. Sander, *Energy Fuels*, 2000, **14**, 1280–1285.

53 P. Sommersacher, T. Brunner and I. Obernberger, *Energy Fuels*, 2012, **26**, 380–390.

54 A. Magdziarz, M. Gajek, D. Nowak-Woźny and M. Wilk, *Renewable Energy*, 2018, **128**, 446–459.

55 S. Link, P. Yrjas, D. Lindberg and A. Trikkel, *ACS Omega*, 2022, **7**, 2137–2146.

56 A. Mlonka-Mędrala, A. Magdziarz, M. Gajek, K. Nowińska and W. Nowak, *Fuel*, 2020, **261**, 116421.

57 J. Yang, Z. Feng, L. Ni, Q. Gao, Y. He, Y. Hou and Z. Liu, *ACS Omega*, 2021, **6**, 7008–7014.

58 Z. Liu, Z. Feng, H. Xiang, J. Yang and J. Zhang, *J. Therm. Anal. Calorim.*, 2021, **146**, 461–468.

59 I. Carević, N. Štirmer, M. Serdar and N. Ukrainczyk, *Materials*, 2021, **14**, 1632.

60 E. Lindström, M. Öhman, R. Backman and D. Boström, *Energy Fuels*, 2008, **22**, 2216–2220.

61 C. W. Bale, P. Chartrand, S. A. Degterov, G. Eriksson, K. Hack, R. B. Mahfoud, J. Melançon, A. D. Pelton and S. Petersen, *Calphad*, 2002, **26**, 189–228.

62 I. Obernberger, Aschen aus Biomassefeuerungen-Zusammensetzung und Verwertung, Inst, *für Verfahrenstechnik, Techn. Univ. Graz*, 1997.

63 T. Keipi, H. Tolvanen, L. Kokko and R. Raiko, *Biomass Bioenergy*, 2014, **66**, 232–239.

64 I. Aigner, C. Pfeifer and H. Hofbauer, *Fuel*, 2011, **90**, 2404–2412.

65 K. Matsuoka, T. Shimbori, K. Kuramoto, H. Hatano and Y. Suzuki, *Energy Fuels*, 2006, **20**, 2727–2731.

66 I. Samprón, F. Luis, F. García-Labiano, M. T. Izquierdo, A. Abad and J. Adánez, *Bioresour. Technol.*, 2020, **316**, 123908.

67 I. I. Ahmed and A. K. Gupta, *Appl. Energy*, 2011, **88**, 1613–1619.

68 I. Sircar, A. Sane, W. Wang and J. P. Gore, *Fuel*, 2014, **119**, 38–46.

69 M. J. Dirbeba and J. Werkelin, *IntechOpen*, 2022.

70 D. Porbatzki, M. Stemmler and M. Müller, *Biomass Bioenergy*, 2011, **35**, S79–S86.

71 P. Nanou, M. C. Carbo and J. H. A. Kiel, *Biomass Bioenergy*, 2016, **89**, 67–77.

72 A. H. H. Janssen and M. C. Carbo , *Deliverable No.* D, 2013, 4, p. 1.

73 D. Thrän, J. Witt, K. Schaubach, J. Kiel, M. Carbo, J. Maier, C. Ndibe, J. Koppejan, E. Alakangas, S. Majer and others, *Biomass Bioenergy*, 2016, **89**, 184–200.

74 ed. J. G. Speight, The Refinery of the Future, Gulf Professional Publishing, 2020, pp. 343–389.

75 S. Link, S. Arvelakis, A. Paist, T. Liliedahl and C. Rosén, *Renewable Energy*, 2018, **115**, 1–5.

76 T. Tobin, R. Gustafson, R. Bura and H. L. Gough, *Biotechnol. Biofuels*, 2020, **13**, 1–16.

77 A. Siciliano, C. Limonti, G. M. Curcio and R. Molinari, *Sustainability*, 2020, **12**, 7538.

78 C. Gilbe, M. Öhman, E. Lindström, D. Boström, R. Backman, R. Samuelsson and J. Burvall, *Energy Fuels*, 2008, **22**, 3536–3543.

79 Y. Zhu, Y. Niu, H. Tan and X. Wang, *Front. Energy Res.*, 2014, **2**, 7.

80 M. Aho and E. Ferrer, *Fuel*, 2005, **84**, 201–212.

81 Y. Niu, H. Tan, X. Wang, Z. Liu, Y. Liu and T. Xu, *Energy Fuels*, 2010, **24**, 2127–2132.

82 A. Uslu, A. P. C. Faaij and P. C. A. Bergman, *Energy*, 2008, **33**, 1206–1223.

83 Y. Li, P. Tittmann, N. Parker and B. Jenkins, *GCB Bioenergy*, 2017, **9**, 681–693.

84 P. Abelha and J. Kiel, *Biomass Bioenergy*, 2020, **142**, 105751.